

Simons Observatory: Observatory Scheduler and Automated Data Processing

Yilun Guan^{a,b}, Kathleen Harrington^{c,d}, Jack Lashner^e, Sanah Bhimani^e, Kevin T. Crowley^f, Nicholas Galitzki^{j,k}, Ken Ganga^g, Matthew Hasselfieldⁱ, Adam D. Hincks^{b,h}, Brian Keating^f, Brian J. Koopman^e, Laura Newburgh^l, David V. Nguyen^e, and Max Silva-Feaver^e

^aDunlap Institute for Astronomy & Astrophysics, University of Toronto, 50 St. George St., Toronto ON M5S 3H4, Canada

^bDavid A. Dunlap Department of Astronomy and Astrophysics, University of Toronto, 50 St. George St., Toronto ON M5S 3H4, Canada

^cHigh Energy Physics Division, Argonne National Laboratory, Lemont, IL 60439, USA

^dDepartment of Astronomy and Astrophysics, University of Chicago, Chicago, IL, 60637, USA

^eWright Laboratory, Department of Physics, Yale University, New Haven, CT 06520, USA

^fDepartment of Physics, UC San Diego, La Jolla, CA 92093 USA

^gUniversité Paris Cité, CNRS, Astroparticule et Cosmologie, F-75013 Paris, France

^hSpecola Vaticana (Vatican Observatory), V-00120 Vatican City State

ⁱCenter for Computational Astrophysics, Flatiron Institute, 162 Fifth Avenue, New York NY, 10010

^jDepartment of Physics, University of Texas at Austin, Austin, TX, 78712, USA

^kWeinberg Institute for Theoretical Physics, Texas Center for Cosmology and Astroparticle Physics, Austin, TX 78712, USA

^lDepartment of Physics, Yale University, New Haven, Connecticut 06520, USA

ABSTRACT

The Simons Observatory (SO) is a next-generation ground-based telescope located in the Atacama Desert in Chile, designed to map the cosmic microwave background (CMB) with unprecedented precision. The observatory consists of three small aperture telescopes (SATs) and one large aperture telescope (LAT), each optimized for distinct but complementary scientific goals. To achieve these goals, optimized scan strategies have been defined for both the SATs and LAT. This paper describes a software system deployed in SO that effectively translates high-level scan strategies into realistic observing scripts executable by the telescope, taking into account realistic observational constraints. The data volume of SO also necessitates a scalable software infrastructure to support its daily data processing needs. This paper also outlines an automated workflow system for managing data packaging and daily data reduction at the site.

Keywords: Simons Observatory, CMB, Scheduler, Pipeline, Automation, Software

1. INTRODUCTION

Over the past few decades, significant experimental progress has been made in measuring the cosmic microwave background (CMB), the oldest light in the universe. This progress has led to an era of precision cosmology, with experiments such as *Planck*,¹ the Atacama Cosmology Telescope (ACT),² the South Pole Telescope (SPT),³ and the BICEP/Keck experiments⁴ achieving unprecedented precision in measuring CMB anisotropies at the level of ten parts per million. These measurements have been the cornerstone of our standard cosmological model, the Λ CDM model, and have placed percent-level constraints on the fundamental properties of our universe. However, key questions remain unanswered, including the existence of primordial gravitational waves from cosmic inflation

Email: yilun.guan@utoronto.ca

and the nature of dark matter and dark energy. To address these questions, next-generation CMB experiments are being built that will offer significantly improved sensitivity in CMB polarization measurements at both small and large angular scales.

The Simons Observatory (SO) is one of the next-generation experiments that will push the frontier in precision measurements of the CMB.⁵ Located in the Atacama Desert at an altitude of 5,200 meters in Chile’s Parque Astronomico, the SO consists of one large aperture telescope (LAT) with a 6-meter primary mirror, and three 0.5-meter small aperture telescopes (SATs). This combination of SATs and LAT enables the SO to make precise measurements of the CMB anisotropies from degree-scale to arcminute-scale. Specifically, the LAT receiver is equipped with around 30,000 transition-edge sensor (TES) bolometric detectors, distributed across seven optics tubes. Each optics tube has three detector modules, each contains a detector wafer that hosts a hexagonal assembly of detector arrays sensitive to two frequency bands. Thanks to the large number of detectors, the LAT can map the CMB sky with arcminute resolution and an approximately 7.8° field of view. In comparison, the mid-frequency (MF; 90/150 GHz) and ultra-high-frequency (UHF; 220/280 GHz) SATs each has around 12,300 detectors installed on seven wafers, fitted in a single optics tube. SAT also features a rotating cryogenic half-wave plate (HWP), which modulates the polarization of incoming light. SAT maps the sky at 0.5° resolution at 93 GHz with a total field of view of around 35° .⁶

The success of the SO in achieving its science goals depends crucially on the development of an optimized scan strategy and observing program.⁷ For SATs, the primary objective is to detect the faint primordial gravitational wave signal in the B-mode polarization, which requires a dedicated scanning strategy that optimizes for noise statistics and foreground cleaning. To achieve this objective, SATs will employ a deep scanning strategy, focusing on small patches of sky with low galactic foreground contamination. In comparison, the LAT will prioritize having large sky coverage, especially in areas that overlap with external surveys such as the Vera C. Rubin Observatory⁸ and the Dark Energy Spectroscopic Instrument (DESI).⁹ This strategy will allow the LAT to effectively probe small-scale anisotropies, including CMB lensing and galaxy clusters, capitalize on joint analysis with these external surveys,¹⁰ and open doors to Galactic science and time-domain science.

With scan strategies defined, the next essential step is to transform the theoretical scan strategies into detailed and executable observing scripts for the telescopes. This is the primary function of the observatory scheduler, responsible for not only effectively executing the main scan strategies but also incorporating a variety of operational requirements essential for instrument health and characterization. These requirements can include scheduling calibration scans using planets, conducting routine IV curve and bias step measurements,* and managing the operations of the HWP. By seamlessly integrating the main scan strategy with the operational needs of the instruments, the observatory scheduler is key to the effective execution of an observing plan, thereby maximizing its observing efficiency. We will provide an overview of the observatory scheduler system in the first part of this paper.

In addition to the observatory scheduler, another critical component of the Simons Observatory’s software infrastructure is the automated workflow system, which is responsible for automating routine data processing tasks. Traditional automated workflow systems, such as `cronjobs`, are commonly used for scheduling script executions at specified times. However, these systems often lack transparency, making it difficult to monitor execution status, inspect logs, and manage task dependencies and concurrency. Furthermore, traditional workflow systems also lack flexibility in controlling execution and its environment.

To overcome these limitations, more modern and robust workflow management tools like Apache Airflow[†] and Prefect[‡] have been invented. These tools are capable of providing a dynamic, extensible, and scalable architecture to manage workflows as directed acyclic graphs of tasks. They also include rich command-line utilities, user-friendly web interface for monitoring task progress, managing dependencies, and much more,

*The IV curve, also known as current-voltage relation, is a key measurement that characterizes the superconducting transition of the TES. It measures the current response of the TES as we vary the voltage applied via the bias lines. The bias step is an alternative method to characterize detectors by measuring the detector’s response to a small-amplitude square-wave added to the bias lines. It measures key calibration parameters such as the resistance of TES, R_{TES} , responsivity, and time constants of the TES.

[†]<https://airflow.apache.org/>

[‡]<https://www.prefect.io/>

Table 1. Example master schedule for the SAT for illustration. Rotation specifies the boresight rotation applied in units of degrees. Az Min/Max specify the boundary of the azimuth scan in units of degrees.

Start Time (UTC)	Stop Time (UTC)	Rotation [°]	Patch	Az Min [°]	Az Max [°]	Elevation [°]
2024-01-01 20:35:00	2024-01-01 21:40:00	-45.00	Patch 1	105.53	145.53	50.00
2024-01-01 21:40:00	2024-01-01 22:45:00	-45.00	Patch 1	105.53	145.53	50.00
2024-01-01 22:45:00	2024-01-01 23:50:00	-45.00	Patch 1	105.53	145.53	50.00
2024-01-01 23:50:00	2024-01-02 00:55:00	-45.00	Patch 2	214.47	254.47	50.00
2024-01-02 00:55:00	2024-01-02 02:00:00	0.00	Patch 2	214.47	254.47	50.00
2024-01-02 02:00:00	2024-01-02 03:05:00	0.00	Patch 2	214.47	254.47	50.00
...

thereby offering a comprehensive and flexible solution for automating complex data processing workflows. SO has adopted **Prefect** to coordinate its daily data processing. **Prefect** stands out because it allows the definition of workflow in Python, which fits naturally with the SO software stack. The Python support also makes it easier to transform the data processing pipelines in SO, as part of the `sotodlib` library,[§] into automated workflows managed by **Prefect**.

Within SO, this **Prefect**-based automated workflow system plays the pivotal role of automating daily data packaging and data reduction pipelines running at the observatory site. The daily data packaging pipeline, specifically, is the critical first step in data analysis at the site which re-bundles low-level data from raw acquisition format into a performance-optimized data structure and resamples relevant housekeeping data to synchronize with the detector timestream to facilitate easier and more efficient downstream data analysis. The workflow system also manages daily data reduction tasks from data preprocessing to, eventually, daily mapmaking, an important prerequisite to the daily transient discovery program in SO. In the second part of this paper we will describe this workflow system in SO and its application in automating data packaging and data reduction pipelines.

This paper will be structured as the following. Section 2 first discusses the general design of the observatory scheduler. Section 3 describes the application of the **Prefect**-based automated workflow system in SO. We conclude in Section 4.

2. OBSERVATORY SCHEDULER

Observation planning in SO is a multi-level process designed to maximize observing efficiency and optimize the respective scientific goals of different instruments. At the highest level, we define different scan strategies for the SATs and the LAT, respectively.

The observatory scheduler is an integral part of the observation planning system in SO, being responsible for transforming a scan strategy into a detailed and executable observing script for the instrument. The input to the observatory scheduler is a so-called *master schedule* that is defined based on the higher-level scan strategy. The master schedule is composed of a set of scan blocks, each of which contains constant elevation scans of a specific sky patch. In SO, we can produce this master schedule using either a “classical” scheduler, or an “opportunistic” scheduler.⁷ The classical scheduler, which will be used during commissioning and early observations, typically orchestrates observations simply by cycling through a pre-defined list of target fields, during both periods when the field is rising and setting in the sky. The opportunistic scheduler on the other hand, like that used in Advanced ACTPol,¹⁰ sub-divides target fields into tiles and dynamically adjusts priorities based on the frequency of visits to each tile, after accounting for observational constraints like Sun avoidance or Moon avoidance. This can be used later for SO, when the various possible systematics which might affect the observations are understood. Table 1 shows an example master schedule, where each row corresponds to an approximately one-hour period of constant elevation scan, parameterized by the target azimuth, elevation, boresight rotation, and the azimuth range of the scan.

Using the master schedule as input, the scheduler first constructs a daily observing plan that adheres to the master schedule while incorporating additional operational requirements, such as the inclusion of calibration

[§]<https://github.com/simonsobs/sotodlib>

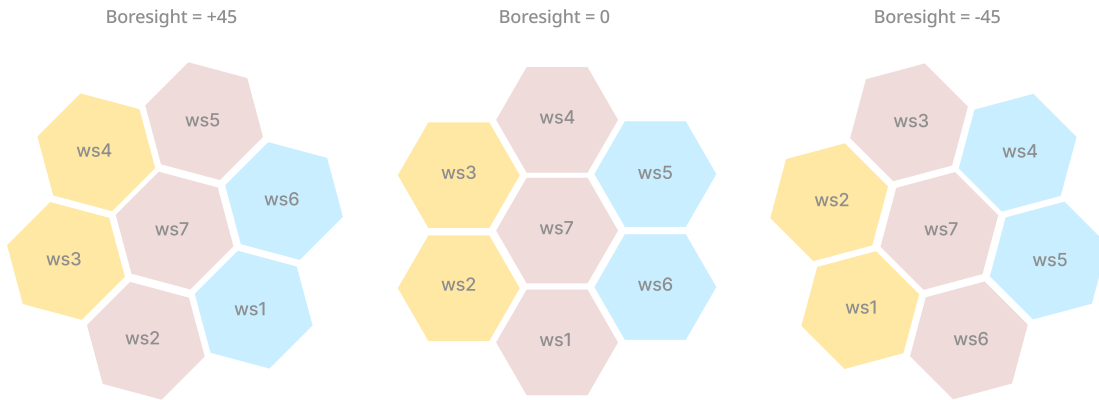


Figure 1. Definition of wafer groups on the SAT focal plane with boresight rotation set to $+45^\circ$, 0° , and -45° , respectively. Three wafer groups are defined as approximately vertical columns, color coded as yellow, red, and blue, respectively. **ws#** denotes a specific wafer slot, where “wafer slot” is a unique identifier for a sub-array location in the full SAT focal plane.

targets essential for determining the pointing offsets of detectors and their relative optical gain. For instance, the SATs require routine calibration using Jupiter and Saturn observations. The scheduler injects these planet targets into the observing plan on a day-to-day basis, depending on the calibration strategy. The entire field-of-view over 30 degrees, which is too large to efficiently scan with sufficient signal-to-noise during a calibration operation. Instead we sub-divide the full focal plane into separate wafer groups, each containing a column of wafers. Figure 1 shows the definition of three wafer groups in the SAT focal plane, at different boresight rotation settings. Wafer groups are typically defined as an approximately vertical column of wafers to minimize the azimuth throw required to cover all detectors in the wafer group. The scheduler supports scheduling planet scans targeting a specific wafer group, thereby improving the scan density of each planet observation and the calibration quality. We discuss the detailed algorithm of planet scan planning in Section 2.1.

In addition to adding planet scans, the scheduler also takes into account various other operational constraints set by the telescope operator. These constraints are defined as *rules* that modify each scan block accordingly. One of the most critical rules is the *sun avoidance* rule, which trims scan blocks so that they do not reach within a pre-defined radius around the Sun, thereby preventing instrument damage. Figure 2 shows an example of a sun avoidance rule being applied to trim both CMB and planet scan blocks. We discuss sun avoidance rules in details in Section 2.2. To facilitate day-to-day operation requirements in an observing day, the scheduler implements a suite of rules, in addition to sun avoidance, that can be turned on when planning observations, such as the azimuth range rule which trims each scan to within a specified azimuth range.

When two scan blocks overlap in time, conflict resolution becomes necessary. In the early stages of SO, we adopt a prioritization policy that favors calibration targets over CMB scans. As a result, CMB scan blocks may be trimmed or split to accommodate calibration scans. However, as our understanding of the instrument evolves and as we start to maximize science outputs, we anticipate this prioritization policy to adapt and change. In the case when two calibration targets conflict in time, the lower priority target, as defined by the remote observer, will be skipped. The skipped calibration target will get a higher priority in the next planet passage. Figure 2 shows an example of conflict resolution where the CMB scan is trimmed to prioritize a Saturn scan.

With the observing plan established, the scheduler’s next step is to break down the plan into a detailed list of operations. These operations include setup procedures at the beginning of an observing session, termed *pre-session* operations, wrap-up procedures at the end of an observing session, termed *post-session* operations, operation sequences that set up the telescope before each scan, such as spinning up the half-wave plate when observing a planet, termed *pre-scan* operations, and follow-up tasks after each scan, such as bias step measurements, termed *post-scan* operations. To observe the targets on schedule, the scheduler must fully account for the

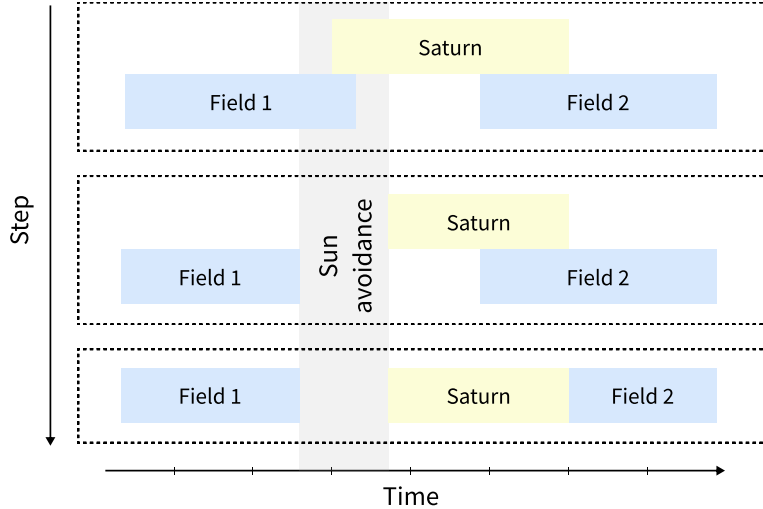


Figure 2. An example observing planning process. In panel 1 we inject a Saturn scan in the master schedule; in panel 2 we trim both the CMB and the planet scans based on the sun avoidance rule; in panel 3 we resolve the scheduling conflict between Saturn scan and cmb scan by prioritizing calibration.

timing of pre- and post-scan operation sequences, which is especially critical for planet observations due to the limited observing window to observe a planet at a given elevation. Planning operations is a non-trivial problem, as it requires careful accounting of various state dependencies and operational constraints. The SO scheduler adopts a multi-pass approach to plan for operations, which we discuss in more detail in Section 2.3.

When scheduling pre- and post-scan operations, it is crucial to ensure the telescope’s safety from the Sun during these operations, which leads to an additional scheduling constraint. A traditional approach would typically restrict these operations to a sun-safe interval, but this may result in the unnecessary loss of valuable observation time. To overcome this issue, the scheduler focuses on identifying alternative sun-safe azimuth positions for the telescope during the pre-scan operations. By selecting a sun-safe azimuth for the duration of the operations, the telescope can maintain a constant elevation for scanning while staying clear of the Sun. Once the pre-scan phase concludes, the telescope moves azimuthally to the desired observing pointing at the scheduled time. This revised strategy improves the total observation time when pre-scan operations are affected by Sun exposure. A more detailed discussion of this approach can be found in Section 2.4.

After establishing the operation plan, the scheduler will translate each operation into a series of Python commands based on the `sorunlib`[¶] Python library, which interfaces with the Observatory Control System.¹¹ Like the operation planning process, the commands generated may be state-dependent. This translation step, therefore, also accounts for the state progression to generate commands that accurately reflect the telescope’s operational states at various times. In addition, the commands generated for each operation are interspersed with `wait` commands, which synchronize the execution of the script with the given operation schedule. The result of this step is an executable Python script composed of `sorunlib` commands. This script is then passed to and executed by the sequencer, `nextline`,¹² an online Python interpreter connected to the observatory control system to facilitate the live control and operation of the observatory.

Figure 3 shows an overview of the scheduling algorithm described above. We refer to this algorithm as our baseline scheduling program. In practice, alternative scheduling programs may be necessary to perform instrument tests or special observations. To support flexibility in switching between different scheduling programs, we maintain a database that associates each program with a specific date range. The sequencer, `nextline`, supports automatic retrieval of a new observing script upon completion of a running one by sending a request to the scheduler. The scheduler then references the database of observing programs to identify an active program for the date requested and redirects the request to the relevant scheduling program to produce an observing script and

[¶]<https://github.com/simonsobs/sorunlib>



Figure 3. Overview of the scheduler’s workflow.

return to `nextline`. This approach has proven particularly useful in the early stages of SO when auto-generated observing scripts are often interspersed with manually-developed scripts by the telescope operators to perform special instrument tests.

2.1 Planet scan

Planet scans are injected into the master observing plan on a day-to-day basis based on instrumentation requirements. With the large focal plane sizes in SO and the short observing window of a planet transit, we typically divide the focal plane into several groups of wafers (wafer groups) and set each planet scan to target one specific wafer group. Figure 1 shows the definition of three wafer groups in the SAT focal plane, as three vertical columns. Such a vertical split minimizes the azimuth throw needed to cover all the detectors, thus improving the scan density and calibration quality. With each planet scan focusing on one wafer group, we need multiple planet transits to fully map the focal plane. This typically takes observations over several days to finish. We define calibration targets as the combination of a planet target, the wafer group, elevation, and, for the case of SAT, the boresight rotations. Table 2 gives an example of a list of calibration targets that can be inserted to the master observing plan.

Table 2. Example calibration targets for SAT: `ws#` stands for specific wafer slot. Rotation refers to boresight rotation to be applied.

Source	Wafer Group	Elevation	Rotation
Jupiter	ws1, ws2	50°	0°
Jupiter	ws2, ws3	50°	45°
Saturn	ws2, ws3	50°	-45°

For a given calibration target, we solve for an optimal scan at a target elevation, el_0 , that minimizes the total observation time needed to cover every detector in the target wafer group with the following steps.

- We first pre-compute the trajectory of the source, $az_s(t)$, $el_s(t)$, for the full time span of the observing plan when the source is above the horizon and split the full observing window based on rising or setting modes. Here az and el represent azimuth and elevation, respectively.

- We parametrize each wafer slot in the target wafer group as a circle in boresight coordinate, (ξ, η) ,[†] and produce dummy detectors that trace the outer boundary of the wafer group, with coordinates (ξ_i, η_i) for the i -th dummy detector. These dummy detectors allow for easy tracking of the apparent geometry changes of each wafer in horizontal coordinates (az, el) at different points on the sky. We refer to these dummy detectors as “detector cover” hereafter.
- We compute the center of the target wafer group as the average of the detector cover, (ξ_w, η_w) , and solve for an azimuth az_0 such that when our boresight is at (az_0, el_0) , the center of the wafer group, (ξ_w, η_w) , falls on the trajectory of the source, $(az_s(t), el_s(t))$. We then calculate the sky coordinates of each detector in the detector cover, (az_i, el_i) when our boresight is at (az_0, el_0) . This step effectively moves the boresight to the target elevation such that the center of the wafer group approximately intersects with the source trajectory.
- We can then easily design an optimal scan for this calibration target. For a rising source, the start time of the scan is, $t_0 = \{t \mid el_s(t_0) = \min\{el_i\}\}$, and the stop time is $t_1 = \{t \mid el_s(t_1) = \max\{el_i\}\}$. The azimuth throw of the scan will go from $az_{\min} = \min\{az_i\}$ to $az_{\max} = \max\{az_i\}$. A setting scan can be planned similarly with the start and stop times reversed.
- SO also supports adding a constant azimuth drift to the scan, introducing $\Delta az(t) = v_{\text{drift}}t$, with v_{drift} a constant drift speed. This has the potential to further reduce the azimuth throw required to cover a target wafer group to improve the observing efficiency and scan density. To build an optimal scan with azimuth drift enabled, we first compute the effective trajectory of the source by subtracting the effect of drift, $(az_{\text{eff},s}, el_{\text{eff},s}) = (az_s - \Delta az, el_s)$, and then perform the same steps as above as if no drift is applied. We repeat this process for different v_{drift} to identify the optimal v_{drift} that minimizes the azimuth throw of the scan using a `scipy` optimizer. Figure 4 shows a comparison between a planet scan solution with azimuth drift enabled and one without for a rising Saturn targeting the central column of wafers. In both solutions, the planet will scan across all detectors in the target wafer group, but with drift enabled, we reduce the azimuth throw required from 40.8° to 27° , thereby increasing the density of the planet scan. As a result, we enable drift mode for all planet observations.

When scheduling multiple calibration targets within one observing session, we at times run into schedule conflicts. Due to the nature of the calibration scan, we avoid trimming a planet scan unnecessarily and favor full coverage of the target wafer group whenever possible. Therefore the scheduler will choose the target with higher priority and discard the overlapping lower-priority target when conflict occurs. To achieve balanced statistics of different calibration targets while obeying provided priority, we use a round-robin scheduling policy for calibration targets:

- We first compute all scan options for each calibration target. Each day we expect to have two options for each target, one when the target is rising in the sky and one when it’s setting.
- We then iterate through the list of calibration targets following the predetermined order. For each calibration target, we iterate through the list of the scan options for this target and inject into the master observing plan the first scan option that doesn’t have a conflicting calibration scan. This scan option will also be removed from the option list. After we exhaust the list of scan options for a target, we discard this target from the target list, and when we have iterated through all calibration targets while there are still unscheduled scan options, we reiterate from the beginning of the list, repeating the same steps until all options are either scheduled or dropped due to scheduling conflicts.
- When the calibration scan conflicts with the baseline CMB scans, on the other hand, we simply trim the CMB scans to make space for calibration scans, as at the early stage of SO we chose to prioritize better characterization of the instrument over maximizing the science outputs.

The effect of this round-robin scheduling policy is that calibration targets that have discarded a scan option due to schedule conflict will have higher priority in scheduling its next scan option.

[†]The coordinate, $\xi = \eta = 0$, corresponds to the boresight center

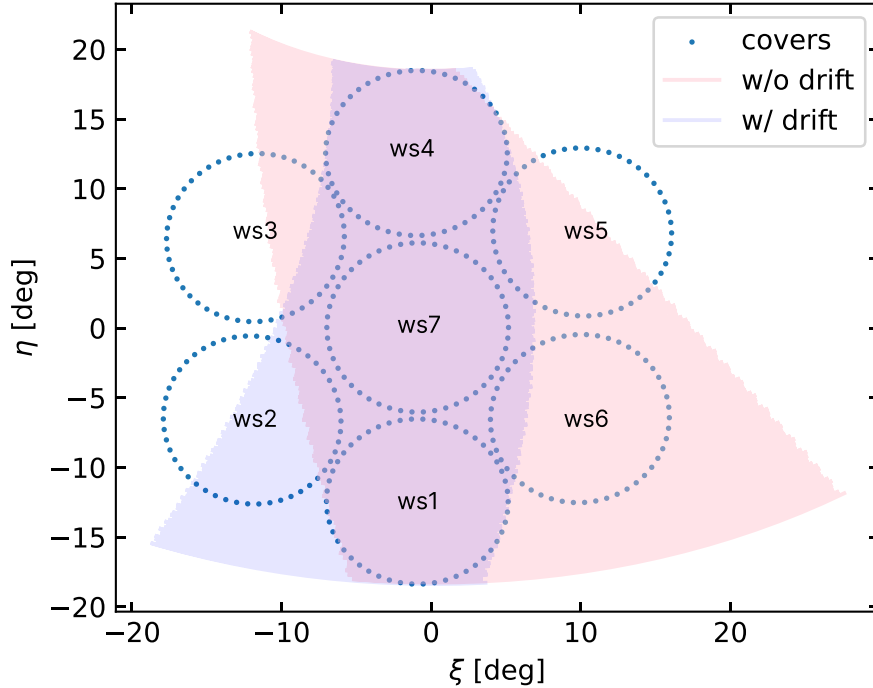


Figure 4. An example Saturn rising scan that targets the central column of wafers (wafer slots: `ws1`, `ws4`, `ws7`). The blue dots represent the detector cover for different wafers. The shaded area represents the trajectory of the planet scan solution in focal plane coordinates. The shaded area in red represents the planet solution without enabling azimuth drift; the shaded area in blue represents that with azimuth drift enabled. When azimuth drift is enabled, the azimuth throw required to cover all detectors in the target wafer group is significantly reduced, from 40.8° to 27.0° .

2.2 Sun avoidance

Direct exposure to sunlight may severely damage our instrument. The scheduler ensures the observing plan is Sun-safe with the following steps.

- For each scan block, we use the start time of the block as a reference time and compute the sky coordinates of the Sun in equatorial coordinates using `pyephem`.**
- We create an empty map in equatorial coordinates covering all possible right ascension and declination reachable by SO. For each pixel of the map, we compute the distance between this pixel and the Sun and store it as a sun distance map.
- We identify pixels that fall within a predefined exclusion radius (41° for SAT) and mask them as Sun-unsafe. Knowing a pixel is Sun-safe at a particular reference time is insufficient as the Sun also drifts on the sky. To calculate how long a pixel will remain Sun-safe, we use the fact that the Sun moves effectively along the axis of right ascension at 0.25 arcminute per second. For a pixel that is 1° away from the nearest Sun-exposed pixel at the same declination, this pixel will remain safe for 240 seconds before entering the exclusion radius from the Sun. We define this duration as the Sun-safe duration.
- We compute the Sun-safe duration for all the pixels, similar to the Sun distance map. For a given block we then compute all pixels that will be covered by the scan, and if any pixel has a Sun-safe duration less than $d + 30$ minutes, with d the duration of the block in minutes, we flag this block as Sun-unsafe and trim it such that no pixels will violate the Sun-avoidance rule. The 30 minutes interval is chosen specifically as a last-resort response time such that when all Sun avoidance procedures have failed, the on-site team will have this amount of time to manually protect the instrument.

**<https://rhodesmill.org/pyephem/>

2.3 Operation planning

With an observing plan established, we need to plan for the time needed for various instrumentation tasks and fully account for the state progression in the schedule. This is especially important for planet scans as observing a planet passage at a target elevation requires an accurate pre-planning to prepare the telescope. As an example, during the early commissioning stage, SATs have the requirement that the HWP should be spinning during a planet scan; we also require the HWP to stop spinning when the telescope elevation is changed to protect the HWP. Suppose spinning up and down the HWP both take 20 minutes. In order to start a planet scan at time t_0 , the minimum time required to prepare the telescope in the required state depends on the state of the system. As illustrated in Table 3, depending on whether the HWP is already spinning and whether an elevation change is necessary, the minimally required setup time before the planet scan varies significantly. HWP operation is one of the many such operations that has a dynamic setup time based on the prior state. It is thus crucial for the scheduler to fully track the state progression during an observing session to observe a planet at the scheduled time.

Table 3. An example of how the detector setup time depends on the state of the telescope.

Case	HWP Status	Elevation Change	Setup Time
1	Spinning	No	0 minutes
2	Not Spinning	No	20 minutes
3	Spinning	Yes	40 minutes
4	Not Spinning	Yes	20 minutes

To track state dependency and the associated time cost for different operations, we define each operation as a function that takes in the observatory state and returns a modified state together with the duration of the operation (i.e., `operation(state) -> (new.state, duration)`). We group operations based on how they are scheduled. Pre-session operations are observatory setup operations scheduled at the beginning of an observing session, which typically lasts a day. Post-session operations are wrap-up operations scheduled at the end of the session. Pre-scan operations include setup tasks performed before each scan block, while post-scan operations are scheduled right after each scan block.

Given the state of the instrument at t_i as s_i , applying an operation, op_i , will progress the state to s_{i+1} with $(s_{i+1}, T_i) = op_i(s_i)$ and increment the clock with $t_{i+1} = t_i + T_i$, where T_i is the duration of operation i . A basic requirement for scheduling a state-dependent operation is that op_i cannot be scheduled before t_i , otherwise the state s_i will no longer be valid. This poses an important causal time constraint during operation scheduling. This constraint requires a strict chronological state progression, and thus leaves little room for prioritization. On the other hand, in practice we often want to prioritize some scans over the others, such as prioritizing calibration scans over the baseline CMB scans in the early stage of SO. To solve this problem we use a multi-pass scheduling approach. The basic idea of this approach is that in the first pass we allow calibration operations to violate the causal constraint and extend into previous non-calibration operations. The invalid state will be corrected in the second pass. In the second pass we first trim the CMB operations that overlap with calibration operations, and then re-schedule all operations with causal constraint to produce an operation plan with valid state progression. A scan that cannot fit into the constrained time window will be skipped.

The detailed steps in the scheduler are as follows:

1. **Initializing the scheduler:** At time t_0 , the scheduler determines the initial state of the instrument, s_0 . It then adds pre-session operations at t_0 and progresses the state and clock to s_1 and t_1 , respectively.
2. **First-pass planning:** Starting at t_1 with state s_1 , we perform the first pass planning by iterating through the list of scans in the observing plan in chronological order. For each scan block, we define a time constraint that specifies the time window in which all operations for the scan should be scheduled. For baseline CMB scans, we use the causal time constraint, and for a calibration scan, we extend the time constraint to whenever the previous calibration operation is scheduled, to avoid conflicting with other calibration operations. We add operations for a scan to the schedule in the order of pre-scan operations, scan operations, and post-scan operations, progressing the state and clock accordingly.

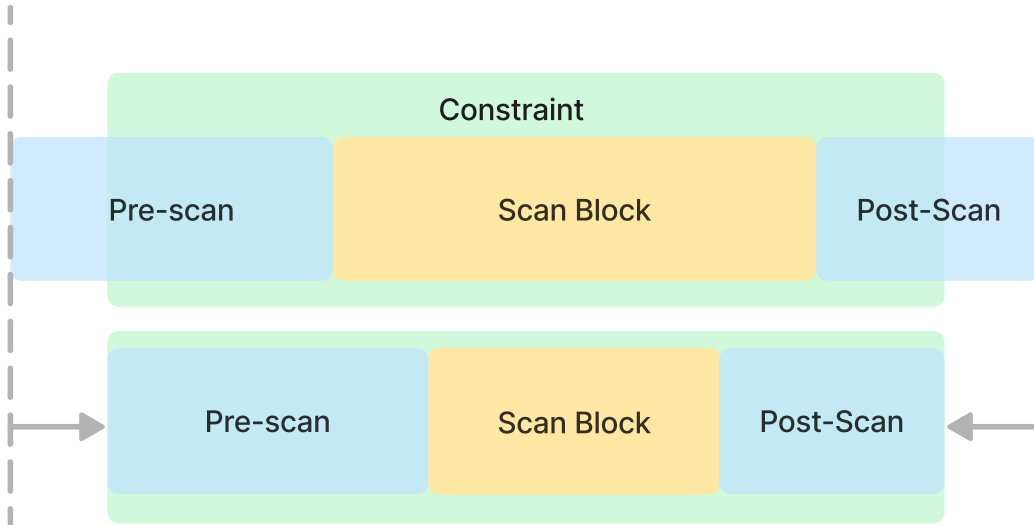


Figure 5. Constrained planning of pre-/post-scan operations.

3. **Optimizing scan operations:** When adding operations for a scan within the time constraint, if the duration of the pre-scan operations is short enough that they finish well before the scheduled time, we update the time constraint based on the estimated gap time, backtrack the state to before the operation, and re-inject the operation to the plan to avoid unnecessary gaps between pre-scan operations and the actual scan operation. In the case that the time constraint does not leave enough time for the pre-scan operations to complete, the scan block will be trimmed to the current clock time. On the other hand, when scheduling a post-scan operation and if the time constraint leaves not enough time to complete the operation, the scan block will be trimmed by the expected excess time, and we will backtrack the state to re-plan the block. Figure 5 illustrates the effect of this constrained planning, where the scan block has to be trimmed to make time for pre- and post-scan operations within time constraint.
4. **Second-pass planning:** In the second pass, we repeat the same steps as the first pass with some important differences in how the time constraint for a scan is set. Specifically, in the second pass, we set the time constraint for CMB scans such that they obey the causal constraint and also do not run into any calibration operations in the future, based on the result of the first pass. For calibration scans, we require simply a causal constraint in the second pass. This second pass will produce an operation plan with valid state progression.

2.4 Azimuth movements

During operation planning, we must ensure that both pre-scan and post-scan operations are safe from direct sunlight exposure. Instead of restricting the time constraints to a sun-safe time window, which can lead to loss of observation time, we employ an alternative approach. While our instrument has strict elevation requirement for pre-scan setup operations, we are flexible to move in azimuth. We can therefore find an azimuth “parking” spot that is sun-safe for the duration of the setup and perform the operations there before moving back to the target azimuth.

For instance, if a particular pointing is sun-safe for 10 minutes, but the expected duration of the pre-scan operations is 20 minutes, we will not be able to observe this target at all if we restrict the pre-scan operations to complete within the sun-safe time. Alternatively, we can find an azimuth that is sun-safe for over 20 minutes, move to this position, perform the operations, and then move back to the target azimuth without losing any observation opportunity. The SO scheduler follows this alternative approach when scheduling pre-scanning operations. Post-scanning at the time of writing is typically instantaneous so we do not move the telescope unnecessarily and restrict the operations to complete within the sun-safe interval of the original scan.

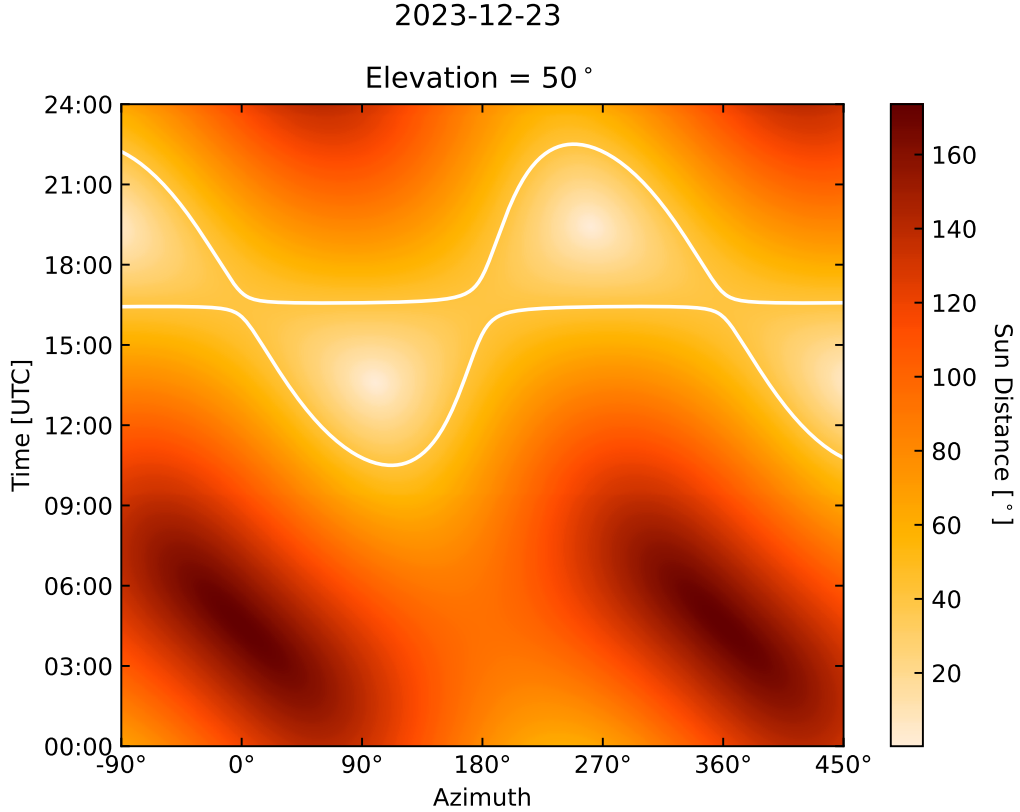


Figure 6. Distance to the sun at various times and azimuths on December 23th, 2023, at 50° elevation. The contour indicates the sun exclusion radius of 41°.

SO platforms can move azimuthally from -90° to 450° . When moving between two points our platform may choose either a clock-wise or counter-clockwise move. During daytime observations, one of the two moves may encounter the Sun in the path. Figure 6 shows an example of how sun distance changes as a function of time and azimuth at 50° elevation. One can easily see that if when moving from 180° to 0° at around 12:00 UTC, we may reach a sun-exclusion zone moving counter-clockwise, whereas if we clockwise move from 180° to 360° , the move is permitted by sun avoidance rule. One also sees that at around 17:00 no azimuth no sun-safe azimuth can be found when observing at this elevation. In cases like this we may either choose to observe at a different elevation, or abort the schedule and stow our telescope.

To find the azimuth move sequence that never reaches a sun-exclusion zone, we consider all possible azimuth move patterns and find an optimized sequence that minimally deviates from the original plan, while ensuring sun-safety of operations and avoiding any motion that would encounter the Sun.

Azimuth planning follows operation planning and involves optimizing the sequence of azimuth moves. We start by iterating through the list of operations. For each pre-scan operation, we calculate the azimuthal ranges that are sun-safe for the duration of the operation. Instead of searching through a fine grid of azimuths, we select a few special values as options. For a pre-scan operation, we consider the boundaries of the azimuth ranges as potential options. If the operation is sun-safe for its duration, we also consider all possible angle unwrappings of the original pointing within the instrument's limit, (-90° to 450°) as options. We assume operations during the actual scan are sun-safe, ensured by previous sun avoidance rule, and consider valid unwrappings of the original pointing as valid options. The reason of these particular azimuth choices will become clear later.

Let $az_i^{(0)}$ denote the original pointing for operation i , and let $az_i^{(j)}$ denote the j -th azimuth option for this operation. We define the best azimuth choice, \tilde{az}_i , for operation i as the one that minimizes the objective

function:

$$\tilde{az}_i = \arg \min_{az_i^{(j)}} \sum_i \left| \text{mod} \left[(az_i^{(j)} - az_i^{(0)}) + \pi, 2\pi \right] - \pi \right|$$

This problem has the structure of a linear programming problem, so we expect the optimal solution to exist at one of the vertices of the feasible region. This is why we consider only a discrete set of azimuth options. To find the optimal azimuth sequence, we recursively explore all possible choices of azimuth for each operation, discarding any path that would encounter the Sun. We then identify the sequence that minimizes the objective function. If such a sequence is found, we assign the resulting azimuth to each operation accordingly. If no safe sequence is found, the schedule reports a failure, indicating to the remote observer that the schedule should be truncated or skipped to avoid the Sun.

3. AUTOMATED WORKFLOW SYSTEM AND AUTOMATED DATA PROCESSING

The massive data volume of SO motivates the development of an automated and scalable data processing pipeline. SO has adopted a modern workflow management system, **prefect**, which is open-source software that offers a robust infrastructure to manage data pipelines at scale. Unlike traditional approaches such as **cronjobs**, **prefect** offers both transparency via online monitoring of running status and logs, and flexibility in managing complex dependencies as well as concurrency requirements, making it an ideal framework to coordinate the automated data pipelines in SO.

The daily data reduction pipeline in SO is modularized into a series of executable scripts with inter-dependencies. To simplify these dependencies, we follow a design choice that each pipeline module should be independently executable and should maintain its own registry of processed datasets and the corresponding data products. We refer to this registry as a manifest database (ManifestDB). Most pipeline scripts that operate over a list of observations maintain their own ManifestDB, which enables the decoupling of complex interdependencies between pipeline modules. As a result, each module can be executed independently in any order, with dependencies resolved through queries to its prerequisite modules' ManifestDBs.

Prefect introduces the concept of a **Flow**, which represents a self-contained, executable unit within a pipeline. This concept integrates with the modular design of SO's data processing pipeline. Moreover, **Prefect** defines a **Deployment** as a **Flow** deployed with specific settings. In SO, we wrap each data processing pipeline module as a distinct **Flow** and create a separate **Deployment** for each telescope, accommodating potential variations in instrument configurations as well as storage locations.

The **Prefect** workflow system allows for the separation of the host environment from the execution environment of flows, enabling remote deployment of flows over a network. In this remote deployment model, flow runs are submitted to a work pool, which distributes the runs among subscribed workers. SO operates two work pools, each responsible for a distinct part of the data processing pipelines. A dedicated compute node is utilized for automated data processing, where pipeline workers are deployed and subscribed to the corresponding work pool. To manage software dependencies, each worker is containerized and deployed using a Docker image,¹³ which provides the necessary software dependencies. A key requirement for scalable data pipelines is concurrency management. To address this, we leverage another **Prefect** feature called **Queue**. Flows that modify the same database are placed on a queue with a concurrency limit of 1, ensuring that data inconsistencies arising from concurrent writes are avoided.

This workflow system is deployed in SO to orchestrate the automated data processing pipelines at the site, which encompasses the critical steps that transform ephemeral data from the detector readout systems, SLAC Microresonator RF (SMuRF) Electronics^{14,15} (referred as SMuRF servers hereafter), into permanent archival data format known as **Books**, perform necessary preprocessing, and, eventually, produce maps of the CMB sky on a routine basis. This full pipeline can be divided into two main stages: data packaging and data reduction.

3.1 Data packaging

The first main stage of the automated data processing pipeline is data packaging. This step is responsible for aggregating and re-bundling raw timestreams from different SMuRF servers and shipping them to long-term data storage sites. A full description of the data packaging is beyond the scope of this paper. Here we provide only a brief overview.

SO employs a three-level process to describe the different life stages of our data, as shown in Figure 7. This process begins with the collection of data by the readout systems. This initial data are saved directly to the SMuRF servers to prevent network outages from causing permanent loss of data. We refer to the data at this stage as level-1 data. Each SO telescope has multiple SMuRF servers so the level-1 detector data are saved across many machines. In the second stage, the level-1 data are aggregated onto the data acquisition (DAQ) nodes for temporary storage. We refer to these aggregated data as level-2. Data at this stage can be broadly classified into two types: SMuRF data and housekeeping (HK) data, with the former accounting for the raw detector timestreams and the latter including ancillary data from supporting hardware such as telescope pointing information, receiver temperatures and pressures, and so on.

Level-2 data are organized and tracked on a per-wafer basis based on the actions commanded to SMuRF (e.g., “stream data”, “take IV curve”), and are stored across multiple files in G3 format, where G3 is a serialized data format developed by SPT-3G¹⁶ adopted as the main data container format for SO.^{††} We register these “level-2 observations” and their associated G3 files in an SQLite database called `G3tSmurf` DB and similarly register the housekeeping (HK) data in a database called `G3tHK` DB. These registries allow for efficient compilation of the cross-wafer observations that correspond to the same physical scan, along with the relevant housekeeping data produced during the same session. This compilation of cross-wafer observations is implemented by a tool called `Imprinter`.

In particular, `Imprinter` registers each set of cross-wafer observations in its own database and initiates the `Bookbinder` process that performs the actual aggregation and re-bundling of G3 files from the multi-wafer observations into a compact format known as a `Book`. Each G3 file is composed of G3 frames which represent the smallest data storage units during reading or writing. Each G3 frame can contain an arbitrarily defined subset of the detector timestreams during data acquisition. The bookbinder also re-divides the G3 frames based on scan patterns such that each frame contains data from a single azimuth sweep. This makes each frame more physically interpretable and more natural to analyze. In addition, `Bookbinder` also catches common data processing failure modes, such as missing samples, missing pointing information, or timing system failures. We refer to the `Books` as level-3 data and consider them to be permanent and immutable data products for long-term storage and data analysis. SO defines five types of `Books` as listed in Table 4.

Table 4. Types of `Books` in the Data Packaging System

Book Type	Description
Observation	Books containing actual measurements of the sky.
Operation	Books recorded during detector operations such as IV measurements or bias steps, containing relevant information for detector characterization.
Housekeeping	Books containing data recorded from the housekeeping feeds.
Stray	A catch-all category for level 2 detector timestreams that do not fit into the above categories.
Smurf	The calibration and metadata output from the various Smurf systems during observations and operations.

Once bound, books are registered and uploaded to the `Librarian` system,¹⁷ which serves as both a bookkeeper and a transport layer, synchronizing the books across all of our data storage sites, including the National Energy Research Scientific Computing Center (NERSC), the Princeton Research Computing Center, and the University of Manchester.

^{††}https://github.com/CMB-S4/spt3g_software

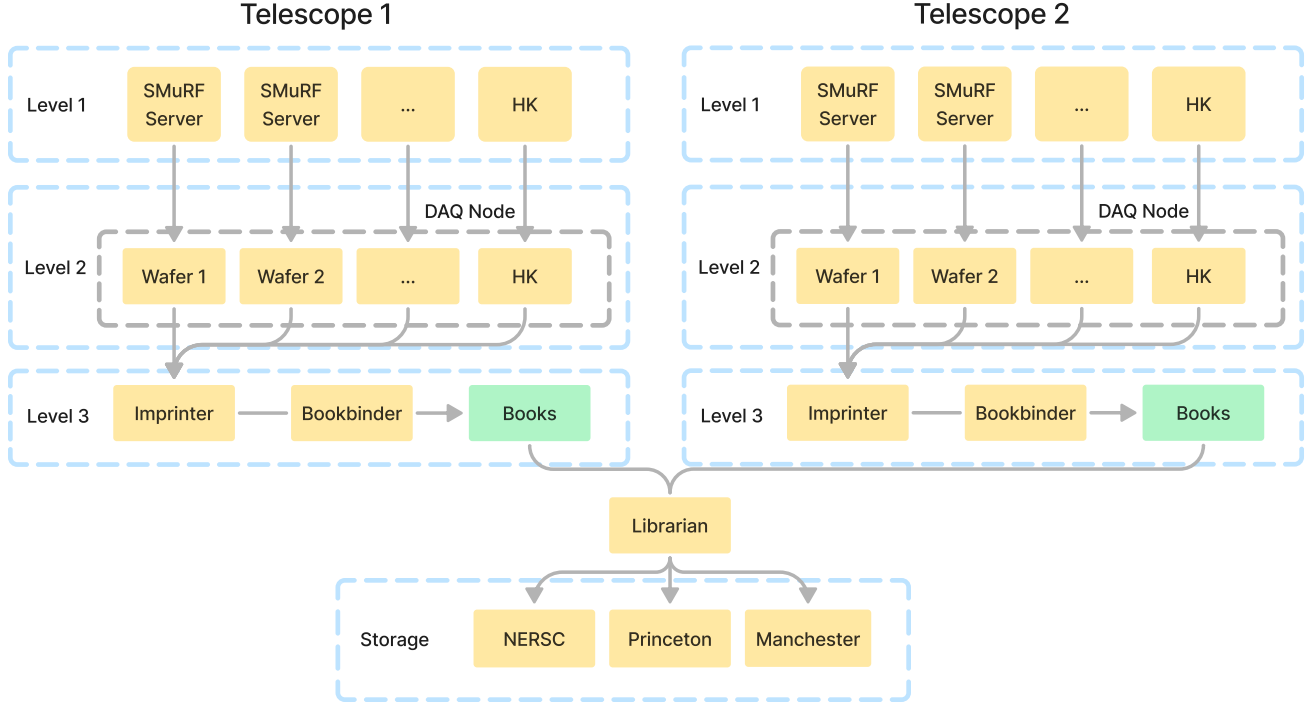


Figure 7. Overview of data packaging pipeline

This data packaging pipeline is coordinated by the **Prefect** workflow system to run automatically. In particular, the pipeline is broken down into five flows, as listed in Table 5, each of which is an independently executable pipeline module responsible for one step in the data packaging pipeline. For example, `update-g3tsmurf-db` and `update-g3tsmurf-hk` flows are responsible for registration of level-2 SMuRF data and housekeeping data, respectively. `update-book-plan` flow implements the `imprinter` and defines the plans for bookbinding, followed by the `make-book` flow which triggers the bookbinder to produce the level-3 books. The last flow, `upload-book`, calls `Librarian` service for book curation and synchronization to remote storage sites.

Table 5. Key data packaging flows managed by the `prefect` automation system.

Module Name	Description
<code>update-g3tsmurf-db</code>	Registration of level-2 SMuRF Observations and the associated G3 files in a local <code>g3tsmurf</code> database.
<code>update-g3thk-db</code>	Registration of housekeeping data in a local <code>g3thk</code> database.
<code>update-book-plan</code>	Definition of book as multi-wafer observation set and register under <code>imprinter</code> database.
<code>make-book</code>	Perform bookbinding based on the definition of books in the <code>imprinter</code> database.
<code>upload-to-librarian</code>	Registration and uploading of books to the <code>Librarian</code> system, which synchronize across storage sites.

3.2 Daily Data Reduction

The second main stage of the automated pipeline in SO is the automated data reduction pipeline, which begins where data packaging ends. Using level-3 books as primary inputs, this pipeline executes a series of data reduction steps, such as detector calibration, matching each detector with its observed resonator frequency (a requirement of the microwave-multiplexing system in SO¹⁸), solving for the HWP angle solution using HWP encoder data, and preprocessing each observation to flag glitches, jumps, and cut bad detectors. These steps are necessary

for achieving daily mapmaking, a crucial target of the data reduction pipeline and a key milestone for time-domain astronomy. Table 6 lists some example data reduction pipeline modules deployed during commissioning. Additional modules, including daily mapmaking, will be integrated in this pipeline in the future.

Table 6. List of data reduction pipeline modules deployed during commissioning. Additional modules including daily mapmaking will be integrated in the future.

Step	Description
<code>update-obs-db</code>	Registration of observations in a database for subsequent pipeline.
<code>make-hwp-solutions</code>	Solve HWP angle solutions.
<code>update-det-match</code>	Match detectors with the observed resonator frequency.
<code>update-smurf-caldbs</code>	Perform detector calibration and store results into calibration databases (CalDBs).
<code>preprocess-tod</code>	Perform preprocessing steps on each <i>Book</i> , including flagging jumps, glitches, bad detectors, and more.

4. CONCLUSION

SO requires optimized observation scheduling to maximize its scientific impacts. This paper presented an overview of the multi-level scheduling process in SO. Optimized scan strategies are designed for each telescope at the highest level to maximize their respective science goals. These scan strategies are then transformed into practical observing scripts that operate the telescope, taking into account detailed instrumentation requirements, such as the injection of calibration scans and additional observing constraints, like sun avoidance rules. The observing plan is subsequently transformed into an operational plan, which accounts for state progression during operations and the expected time cost of each operation. This optimized multi-level scheduling process enables effective realization of the optimized scan strategy while adapting to instrumentation requirements during day-to-day operations.

SO will collect a vast amount of data to achieve the highest precision CMB maps. We need both scalable and automated data processing pipeline at the site to effectively handle this large volume of data. The data processing pipeline at the site involves both data packaging and daily data reduction, starting from the aggregation of ephemeral data from the readout servers up to the daily production of maps. In this paper, we described an automated workflow system deployed at the site, which coordinates the automated data pipelines at the site. This workflow system, based on the open-source `prefect` system, offers several advantages over traditional tools like `cronjobs`, such as transparency of running jobs, flexibility of deployment, and concurrency handling. We have successfully applied this system to coordinate automated data packaging at the site, including the re-bundling of multi-wafer observations into compact `Books` and transporting them to external storage sites. Additionally, this workflow system also manages the daily data reduction pipeline, which includes daily generation of data cuts, jump fixes, and HWP solutions, with the goal of automating daily mapmaking in the near future.

ACKNOWLEDGMENTS

This work was supported in part by a grant from the Simons Foundation (Award #457687, B.K.). YG acknowledges the support from the Dunlap Institute for the duration of this work. The Dunlap Institute is funded through an endowment established by the David Dunlap family and the University of Toronto. ADH acknowledges support from the Sutton Family Chair in Science, Christianity and Cultures, from the Faculty of Arts and Science, University of Toronto, and from the Natural Sciences and Engineering Research Council of Canada (NSERC) [RGPIN-2023-05014, DGEER-2023-00180]. We acknowledge various open source software packages, including `numpy`, `pyephem`, `jax`, `prefect`, which have been instrumental in this work.

REFERENCES

- [1] Ade, P. A., Aghanim, N., Armitage-Caplan, C., Arnaud, M., Ashdown, M., et al., “Planck 2013 results. XVI. Cosmological parameters,” *Astronomy and Astrophysics* **571**, A16 (nov 2014).

- [2] Aiola, S., Calabrese, E., Maurin, L., Naess, S., Schmitt, B. L., et al., “The Atacama Cosmology Telescope: DR4 maps and cosmological parameters,” *JCAP* **2020**, 47 (dec 2020).
- [3] Benson, B. A., Ade, P. A. R., Ahmed, Z., Allen, S. W., Arnold, K., et al., “SPT-3G: A Next-Generation Cosmic Microwave Background Polarization Experiment on the South Pole Telescope,” (jul 2014).
- [4] Ade, P. A. R., Ahmed, Z., Amiri, M., Barkats, D., Thakur, R. B., et al., “BICEP/Keck XV: The BICEP3 Cosmic Microwave Background Polarimeter and the First Three-year Data Set,” *ApJ* **927**, 77 (Mar. 2022).
- [5] Ade, P., Aguirre, J., Ahmed, Z., Aiola, S., Ali, A., et al., “The Simons Observatory: Science goals and forecasts,” *Journal of Cosmology and Astroparticle Physics* **2019**(2) (2019).
- [6] Galitzki, N., Tsan, T., Spisak, J., Randall, M., Silva-Feaver, M., Seibert, J., Lashner, J., et al., “The Simons Observatory: Design, integration, and testing of the small aperture telescopes,” *arXiv e-prints*, arXiv:2405.05550 (May 2024).
- [7] Stevens, J. R., Goeckner-Wald, N., Keskitalo, R., McCallum, N., et al., “Designs for next generation CMB survey strategies from Chile,” in [*Millimeter, Submillimeter, and Far-Infrared Detectors and Instrumentation for Astronomy IX*], Zmuidzinas, J. and Gao, J.-R., eds., *Society of Photo-Optical Instrumentation Engineers (SPIE) Conference Series* **10708**, 1070841 (July 2018).
- [8] LSST Science Collaboration, Abell, P. A., Allison, J., Anderson, S. F., Andrew, J. R., et al., “LSST Science Book, Version 2.0,” (November) (2009).
- [9] DESI Collaboration, Aghamousa, A., Aguilar, J., Ahlen, S., Alam, S., Allen, L. E., Allende Prieto, C., Annis, J., Bailey, S., Bland, C., and et al., “The DESI Experiment Part I: Science, Targeting, and Survey Design,” *arXiv e-prints*, arXiv:1611.00036 (Oct. 2016).
- [10] De Bernardis, F., Stevens, J. R., Hasselfield, M., et al., “Survey strategy optimization for the Atacama Cosmology Telescope,” in [*Observatory Operations: Strategies, Processes, and Systems VI*], Peck, A. B., Seaman, R. L., and Benn, C. R., eds., *Society of Photo-Optical Instrumentation Engineers (SPIE) Conference Series* **9910**, 991014 (July 2016).
- [11] Koopman, B. J. et al., “The Simons Observatory: deployment of the observatory control system and supporting infrastructure,” in [*Software and Cyberinfrastructure for Astronomy VIII*], *Society of Photo-Optical Instrumentation Engineers (SPIE) Conference Series* **13101** (2024).
- [12] Sakuma, T., Guan, Y., Hasselfield, M., Koopman, B., Newburgh, L., and Nguyen, D., “Nextline,” (Oct. 2020).
- [13] Merkel, D., “Docker: lightweight linux containers for consistent development and deployment,” *Linux journal* **2014**(239), 2 (2014).
- [14] Henderson, S. W. et al., “Highly-multiplexed microwave SQUID readout using the SLAC Microresonator Radio Frequency (SMuRF) electronics for future CMB and sub-millimeter surveys,” in [*Millimeter, Submillimeter, and Far-Infrared Detectors and Instrumentation for Astronomy IX*], Zmuidzinas, J. and Gao, J.-R., eds., *Society of Photo-Optical Instrumentation Engineers (SPIE) Conference Series* **10708**, 1070819 (July 2018).
- [15] Yu, C., Ahmed, Z., Frisch, J. C., Henderson, S. W., Silva-Feaver, M., et al., “SLAC microresonator RF (SMuRF) electronics: A tone-tracking readout system for superconducting microwave resonator arrays,” *Review of Scientific Instruments* **94**, 014712 (Jan. 2023).
- [16] Sobrin, J. A. et al., “The Design and Integrated Performance of SPT-3G,” *ApJS* **258**, 42 (Feb. 2022).
- [17] Borrow, J. et al., “Making research data flow with python,” *SciPy 2024 Proceedings* (in prep).
- [18] McCarrick, H., Healy, E., et al., “The Simons Observatory Microwave SQUID Multiplexing Detector Module Design,” *ApJ* **922**, 38 (Nov. 2021).